Biochimica et Biophysica Acta, 511 (1978) 125—140

BBA 78083

PROPERTIES AND THE LOCATIONS OF A SET OF FLUORESCENT PROBES SENSITIVE TO THE FLUIDITY GRADIENT OF THE LIPID BILAYER

KEITH R. THULBORN and WILLIAM H. SAWYER

Russell Grimwade School of Biochemistry, University of Melbourne, Parkville, Victoria, 3052 (Australia)

(Received November 28th, 1977)

Summary

The synthesis and properties of a set of four fluorescent probes (*n*-(9-anthroyloxy) fatty acids, $n = 2, 6, 9, 12$) sensitive to the fluidity gradient of the lipid bilayer are described. Flurorescent quenching experiments show that the probes locate at a graded series of depths in the bilayer. A fifth probe, methyl-9-anthroate, locates near the bilayer centre. As an example of their application, the probes are used to study the phase transitions of dipalmitoyl phosphatidylcholine. Changes in the rotational relaxation times of the probes across the transitions are more pronounced at the centre of the bilayer than at the surface.

Introduction

The acyl chains of phospholipid molecules in a lipid bilayer undergo anisotropic motion about an axis perpendicular to the membrane surface [1]. The rate and amplitude of this motion increases as the terminal methyl group of the chain is approached. The term membrane fluidity encompasses the concept of packing as determined by the average configuration of the acyl chain, as well as the concept of motion as determined by the rate of movement of the acyl chains. Non-perturbing techniques such as ^{2}H NMR and ^{13}C NMR have provided valuable information on the amplitude and rate of motion of the acyl chains in model membrane systems [2,3]; however, their application to natural membranes is restricted because of a lack of sensitivity or because of the complexity of the spectra involved. In natural membranes the use of spectroscopic

Abbreviations: 2-AP, 2-(9-anthroyloxy) palmitic acid; 6-AS, 6-(9-anthroyloxy) stearic acid; 9-AS, 9-(9-anthroylloxy) stearic acid; 12-AS, 12-(9-anthroyloxy) stearic acid; M-9-A, methyl-9-anthroate, A-9-C, anthracene-9-carboxylic acid.

probes has been more rewarding although they also suffer certain disadvantages. For example, nitroxyl-labelled fatty acids have proved useful ESR probes [4] but their usefulness is restricted because their time-dependent reduction in natural membrane systems sometimes requires the presence of an oxidizing agent [5].

Fluorescent probes couple great sensitivity with benefits which may accrue from studies of polarization, quenching and energy transfer reactions [6,7]. However, fluorescent probes such as 1-anilino-8-naphtalene sulfonate and diphenylhexatriene have the disadvantage that their position in the bilayer is not known with certainty. Indeed, any change in the fluorescent characteristics of these probes in membranes may indicate either a change in probe position or a genuine change in bilayer structure [8]. Our approach to this problem has been to synthesize a series of fluorescent fatty acids in which an anthracene group has been attached by an ester linkage to various positions along the acyl chain. Two such derivatives have been reported previously, namely 2-(9-anthroyloxy) palmitic acid (2-AP) and 12-(9-anthroyloxy) stearic acid (12-AS) [9,10]. We have now added two more probes to this series (6-AS and 9-AS) and have used a molecule containing the same fluorophore, namely, methyl-9-anthroate (M-9-A) to probe the environment at the centre of the bilayer. In a previous communication we have reported the fluidity gradient as determined by this set of five probes and have shown that the results agree with those obtained by a non-perturbing technique such as deuterium NMR [11].

We now discuss the fluorescent characteristics of these probes and show that they report the environment at a graded series of depths from the surface to the centre of the bilayer.

Materials and Methods

12-Hydroxystearic acid and 2-hydroxypalmitic acid were purchased from Koch-Light Labs. and the 6- and 9-hydroxystearic acids were obtained from Nu-Chek Prep. Inc. Anthracene-9-carboxylic acid (A-9-C) and trifluoroacetic anhydride came from the Aldrich Chemical Co. Inc. Solvents used in the syntheses were analytical grade, and spectroscopic work employed spectroscopic grade *n*-hexane and methanol. Phospholipids were purchased from Koch-Light Labs. (dipalmitoyl phosphatidylcholine) and Lipid Products (egg phosphatidylcholine). Dimyristoyl phosphatidylcholine was synthesized by the method of Robles and van den Berg [12]. All phospholipids moved as a single spot on thin-layer chromatography.

Preparation of liposomes. The phospholipid was dried as a film on the walls of a 25 ml conical flask and placed under vacuum overnight. Glass distilled water (20 ml) was added to give a lipid concentration of 0.5 mM. For quenching experiments, the dimyristoyl phosphatidylcholine dispersion was sonicated for 4 min under N_2 and the liposomes were annealed at 30° C for 30 min before the addition of probe [13]. Multilayered dipalmitoyl phosphatidylcholine liposomes for the phase transition experiments were prepared by heating the suspension to 45° C for 2 min followed by vortexing for 1 min in the presence of glass beads. The heating and vortexing cycle (1 min each) was repeated five times. Dispersions were maintained below the phase transition temperature for

at least 2 h prior to use. Probes were added in a small volume of methanol (10 μl) and uptake was complete within 2 h as judged by fluorescence intensity and polarization measurements. Binding experiments indicated that at the probe to phospholipid rates employed (1 : 400) all was bound to the lipid phase. The pH of dispersions was within the range 6.80—6.90.

Fluorescence. Steady-state fluorescence measurements were made with a Hitachi-Perkin-Elmer MPF3 spectrofluorometer equipped with a thermostated cell block and polarization accessory. For polarization measurements the intensities of the horizontal and vertical components of the emitted light ($I_\parallel$ and $I_\perp$) were corrected for the contribution of scattered light determined independently for an unlaballed reference solution of the same composition. Thus:

$$p = \frac{(I_\parallel - I_\parallel^S) - G(I_\perp - I_\perp^S)}{(I_\parallel - I_\parallel^S) + G(I_\perp - I_\perp^S)} \tag{1}$$

where p is the polarization and G the grating correction factor.

Phase transitions were measured with an instrument constructed in this laboratory and based on the design of Bashford et al. [9]. Light from a 150 W xenon arc was passed through a calibrated grating monochromator (Metrospec) and the emitted light was isolated with interference filters (460 nm, band width at half maximal transmittance 60 nm). The intensities of $I_\parallel$ and $I_\perp$ were measured simultaneously by two matched photomultipliers (EMI 5914A) placed either side of the cuvette. The photomultiplier response was linear within the range of intensities measured, and the matching of the photomultipliers was checked by measuring the signals as a function of the monochromator slit width. The output signals were automatically corrected for the scatter contribution with backoff potentiometers adjusted for an unlabelled suspension of the same composition. Signals were processed in an analogue circuit to provide a direct readout of polarization and intensity ($= T_\parallel + 2I_\perp$) these being recorded as a function of temperature on two X-Y recorders. Temperature was read by a temperature transducer (National LX5600) placed above the light path in the cuvette. The three output signals (p, I and temperature) were also recorded on paper tape using a data logging system. Rotational relaxation times (ρ) were calculated according to the Perrin equation [14] for isotropic rotation:

$$\left(\frac{1}{p} - \frac{1}{3}\right) = \left(\frac{1}{p_0} - \frac{1}{3}\right)\left(1 + \frac{3\tau}{\rho}\right) \tag{2}$$

where p_0 is the limiting polarization in the absence of rotational motion and τ is the average lifetime of the excited state. Values of p_0 were obtained from Perrin plots of data for the temperature dependence in glycerol solutions [15]. Eqn. 2 provides values of an apparent rotational relaxation time since the rotational motion of the fluorophore in the bilayer is unlikely to be isotropic. Similarly, we have not converted data to values of microviscosity due to the difficulties of choosing suitable viscosity standards and the assumptions involved in making this transformation [16].

Quantum yields were determined by the method of Parker and Ress [17] using quinine sulphate as the standard. Absorbances were maintained below 0.08 to avoid concentration quenching, and samples in methanol were purged with high purity nitrogen to avoid oxygen quenching. Spectra were not cor-

rected for lamp and photomultiplier variation with wavelength and the quantum yields reported can only be used for internal comparison.

Quenching experiments with Cu(II) were carried out at 20°C as follows. A cuvette containing 0.5 mM dimyristoyl phosphatidylcholine liposomes with 5 μM probe was titrated with 5 μl aliquots of $CuSO_4$ (1.24 mM). The quenching showed little time dependency. All intensities were corrected for dilution and light scatter. Quenching experiments with *N,N*-dimethylaniline were carried out in a similar manner. Quenching with 16-nitroxide stearate showed time dependency, and intensities were read when they had levelled off 1 h after addition of each aliquot of quencher.

Lifetime measurements were made with an Ortec nanosecond spectrometer. A combination of 400 and 420 nm cutoff filters effectively prevented scattered light from reaching the photon counter. Neutral density filters were used to avoid pulse build-up by ensuring that less than 2% of total lamp pulses resulted in counted pulses. The performance of the instrument was checked against a standard of quinine sulphate. Results were deconvoluted as single exponentials using a nonlinear least squares fitting program devised by Mr. R. Robbins.

Absorption spectra were measured at 20°C with a Cary 17 spectrophotometer. Infrared spectra were measured with a Perkin-Elmer 457 grating infrared spectrophotometer using KBr discs for samples dried in vacuo for 30 h.

Preparation of fluorescence probes. Probes were synthesized according to the method of Lenard et al. [18] using the appropriate hydroxy fatty acid and trifluoroacetic anhydride-activated A-9-C. The purity of the hydroxy fatty acids and the positions of the hydroxyl groups along the acyl chain was verified by ^{13}C NMR using a combination of chemical shift and longitudinal relaxation time (T_1) measurements and mass spectroscopy (Johns et al., in preparation). M-9-A was synthesized and purified by the method of Parish and Stock [19]. The fluorescent fatty acids were purified by preparative thin-layer chromatography on Kieselgel G Type 60 plates. The 6-, 9- and 12-AS derivatives were separated from reaction by-products and unreacted A-9-C using a solvent of hexane/chloroform/methanol (5 : 5 : 1, v/v). For 2-AP the solvent was chloroform/methanol/water (25 : 10 : 1, v/v). The band containing the probe was scraped off, eluted with acetone or chloroform/methanol (1 : 1, v/v), concentrated and recrystallized from *n*-hexane at 0°C as a white solid. Samples were stored in vacuo in the dark. Purity was checked by thin-layer chromatography on precoated plates (Merck, Kieselgel 60F 254) in both the above solvent systems using ultraviolet light to visualize the fluorescent species and iodine vapour to check for non-fluorescent contaminants.

Theory

The quenching of an excited fluorophore in free solution is expected to follow the Stern-Volmer [20] equation

$$\left(\frac{I_0}{I}\right) - 1 = k_q \tau [Q] \tag{3}$$

where I and I_0 are the fluorescence intensities in the presence and absence of quencher, k_q is the Stern-Volmer quenching constant and $[Q]$ is the concen-

tration of quencher. In this study we shall consider the quenching of the anthracene fluorophore situated in the lipid phase. Thus for a quenching molecule which either partitions into or binds to pre-existing sites in the lipid bilayer, the value of $[Q]$ required may be taken to the first approximation as the concentration of Q in the lipid phase.

Partition. The distribution of a quenching molecule between aqueous (A) and lipid (L) phases may be described by a partition coefficient $K_p = [Q_L]/[Q_A]$. Thus the Stern-Volmer equation becomes

$$\left(\frac{I_0}{I}\right) - 1 = k_q \tau K_p [Q_A] \tag{4}$$

Since $[Q_L]$ and $[Q_A]$ are linear functions of the concentration of quencher in the total volume $V_T = (V_A + V_L)$, Stern-Volmer plots of $(I_0/I) - 1$ versus $[Q_T]$ remain linear. Since

$$V_T[Q_T] = V_A[Q_A] + V_L[Q_L] \tag{5}$$

Eqn. 4 becomes

$$\left(\frac{I_0}{I}\right) - 1 = \frac{k_q \tau K_p V_T [Q_T]}{V_A + V_L K_p} \tag{6}$$

Thus, when $[Q_T]$ is used on the abscissa of the Stern-Volmer plot instead of $[Q_L]$ the slope is given by $k_q \tau K_p V_T/(V_A + V_L K_p)$.

Binding. When a quencher binds to equivalent and non-interacting sites on a lipid membrane according to the reaction, $LQ_{i-1} + Q \rightleftharpoons LQ_i$ $(i = 1, 2, ..., q)$, the amount bound is described by the binding equation [21]:

$$[Q'_L] = [Q_T] - [Q'_A] = \frac{qK_A[L_T][Q'_A]}{1 + K_A[Q'_A]} \tag{7}$$

where K_A is the intrinsic association constant, $[L_T]$ is the total concentration of lipid and the primed symbols $[Q'_A]$ and $[Q'_L]$ refer to concentrations of quencher relative to the total volume. The use of $[Q'_A]$ and $[Q'_L]$ rather than the concentrations in each phase $[Q_A]$ and $[Q_L]$) is valid when $V_A >> V_L$. The concentration of quencher in the lipid phase is now

$$[Q_L] = \frac{[Q'_L]V_T}{V_L} = \frac{V_T q K_A [L_T][Q'_A]}{V_L(1 + K_A[Q'_A])} \tag{8}$$

and the Stern-Volmer equation becomes

$$\left(\frac{I_0}{I}\right) - 1 = \frac{V_T k_q \tau q K_A [L_T][Q'_A]}{V_L(1 + K_A[Q'_A])} \tag{9}$$

Eqns. 8 and 9 have two important consequences which are demonstrated in the simulated example depicted in Fig. 1. Firstly, the concentration of quencher in the lipid phase can be very much higher than the concentration of quencher in the total volume with the consequence that the quenching efficiency can be appreciable at very low quenching concentrations (Fig. 1; upper and lower abscissa scales). Secondly when $[Q_T]$ is used on the abscissa of the Stern-Volmer plot instead of $[Q_L]$ or $[Q'_L]$, the plot becomes non-linear. At high values of $[Q_T]$, binding sites become saturated and further increases in $[Q_T]$ do

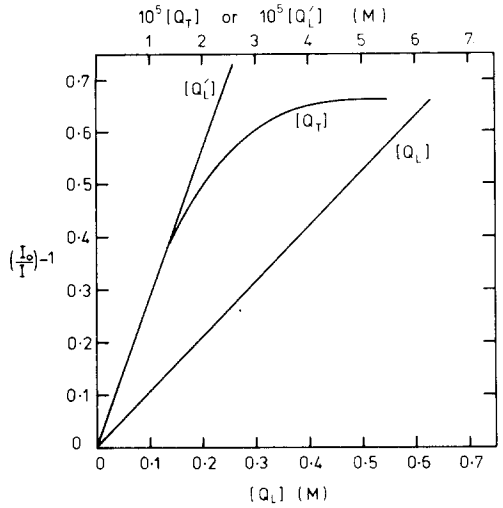

Fig. 1. Simulated Stern-Volmer plots resulting from the binding of a quencher to an acceptor proximal to a fluorophore in or on a membrane. Symbols are defined in the text (see Theory). Values of the constants used in the simulation were as follows: $[L_T] = 50\ \mu M$, $q = 0.5$, $K_A = 1 \cdot 10^6\ M^{-1}$, $k_q = 1 \cdot 10^8\ M^{-1} \cdot s^{-1}$, $\tau = 10.5$ ns. V_T was calculated from the partial specific volume (0.984 ml/g) and the molecular weight (770) of the phospholipid.

not increase quenching. At low values of $[Q_T]$, $[Q'_L] \simeq [Q_T]$ and thus limiting slopes in this region are similar and approach $V_T k_q \tau / V_L$. In double reciprocal form Eqn. 9 is

$$\frac{I}{I_0 - I} = \frac{V_L}{V_T k_q \tau q [L_T] K_A} \cdot \frac{1}{[Q'_A]} + \frac{V_L}{V_T k_q \tau q [L_T]} \tag{10}$$

Thus, the double reciprocal plot ($I/(I_0 - I)$ versus $1/[Q'_A]$) is linear, and K_A = intercept/slope.

Results

Characterization of fluorescent probes

Preparation. Successive recrystallization of the *n*-(-anthroyloxy) fatty acids from *n*-hexane failed to remove traces of the major contaminant, A-9-C. Thin-layer chromatography followed by recrystallization proved a superior purification procedure. The R_F values were similar for 6-, 9- and 12-AS but a lower value was obtained for 2-AP (Table I).

TABLE I

R_F VALUES OF FLUORESCENT PROBES

Solvent	2-AP	6-AS	9-AS	12-AS	M-9-A	A-9-C
A *	0.21	0.50	0.50	0.50	0.73	0.05
B **	0.63	0.82	0.82	0.82	0.87	0.29

* Hexane/chloroform/methanol (5 : 5 : 1, v/v).
** Chloroform/methanol/water (25 : 10 : 1, v/v).

TABLE II

THE DISTINGUISHING INFRARED STRETCHING FREQUENCIES OF FLUORESCENT FATTY ACIDS AND OF MATERIALS USED IN THEIR SYNTHESIS

Species	Carbonyl γ(C = O) (cm^{-1})	Aromatic γ(C — H) (cm^{-1})	Aliphatic γ(C — H) (cm^{-1})
A-9-C	1680	3050	—
M-9-A	1730	3050	—
12-Hydroxystearic acid	1700	—	2850, 2875, 2920, 2960
12-AS	1712	3050	
2-Hydroxypalmitic acid	1745	—	
2-AP	1710	3050	

Infrared specta. The infrared characteristics of 6-, 9- and 12-AS were similar at least in major distinguishing features (Table II). The acyl ester and the aliphatic carboxylic acid carbonyl stretching frequencies were not resolved. However, the single band 1712 cm^{-1} was intermediate between that found for 12-hydroxystearic acid (1700 cm^{-1}) and M-9-A (1730 cm^{-1}) (Table II, column 1). Esterification of the carboxylic group in M-9-A shifted the carbonyl frequency from 1680 to 1730 cm^{-1} as expected. The appearance of the aromatic C-H stretching mode with the fatty acid aliphatic C-H stretching frequency confirms the linkage of the fluorophore to the fatty acid (Table II).

The 2-hydroxypalmitic acid and 2-AP spectra were more complex possibly due to interactions between hydroxyl and carboxyl, and ester and carboxyl groups, respectively. The high carbonyl frequency would be expected for a secondary alcohol with an electronegative group in the α-position, and esterification would explain the observed decrease in frequency compared to other probes. The appearance of aromatic and aliphatic C-H frequencies again confirmed the linkage between the fluorophore and the palmitoyl chain.

Absorption and fluorescence spectra. (Figs. 2 and 3). Both spectra provide

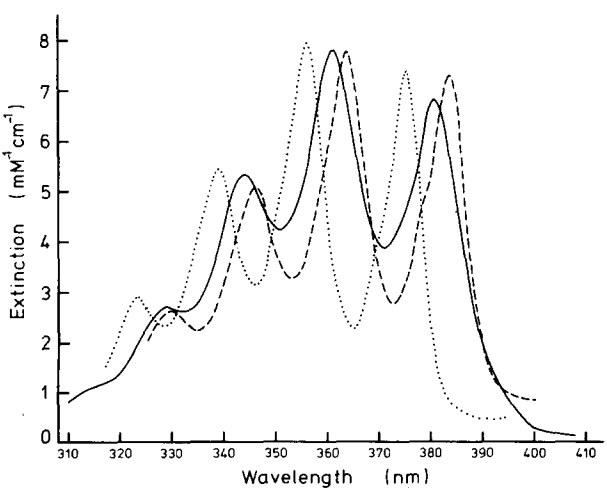

Fig. 2. Absorption spectra of 12-AS (———), anthracene-9-carboxylic acid (— — —) and anthracene (· · · · · ·) in methanol at 20°C.

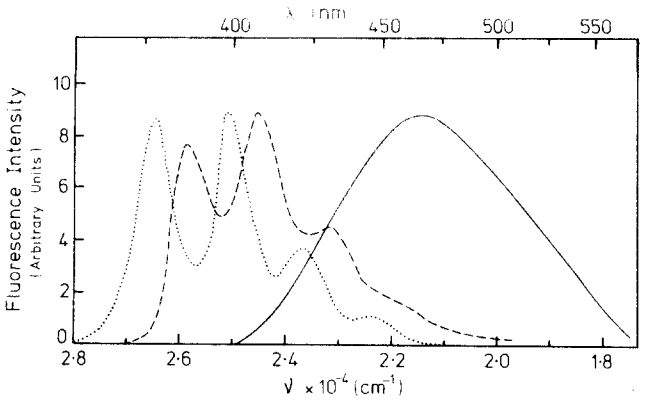

Fig. 3. Uncorrected fluororescence emission spectra of 12-AS (———), anthracene-9-carboxylic acid (— — —) and anthracene (· · · · · ·) in methanol at 20°C. Excitation was at 365 nm and excitation and emission slit widths were 10 and 5 nm, respectively.

useful criteria of purity. The absorption spectrum of A-9-C is blue shifted on esterification to the same extent for all probes. The spectrum of anthracene is blue shifted to a far greater extent. Small amounts of either impurity would be evident as shoulders on the respective peaks, and no such shoulders were observed for the probes purified as described above. The emission spectra of the fluorescent fatty acids in methanol consist of a broad structureless band in contrast to that for anthracene and A-9-C which show distinct structure (Fig. 3).

Table III summarizes the spectral properties of the probes. Within experimental error, all have the same limiting polarization ($p_0 = 0.29 \pm 0.008$). The Perrin plots for the fatty acid probes in glycerol were superimposable, whereas that for methyl-9-anthroate had a significantly steeper gradient (α lifetime/

TABLE III

SPECTRAL CHARACTERISTICS OF FLUORESCENT PROBES

Probe	ϵ [a] ($M^{-1} \cdot cm^{-1}$)	τ (ns) *n*-hexane	τ [b] (ns)	Q [c] methanol	Q [d]	λ_{max} (nm) [e]			
						H_2O	Methanol	*n*-Hexane	Liposomes [f]
2-AP	6730 ± 140	11.0	7.7	—	0.34	455	457	445	451
6-AS	8280 ± 120	10.6	8.7	0.071	0.53	452	461	445	447
9-AS	7860 ± 220	10.4	9.5	0.071	0.51	446	461	446	447
12-AS	7770 ± 20	10.5	10.4	0.071	0.74	452	458	446	446
M-9-A	7110 ± 240	12.1	10.9	0.071	0.44	480	461	447	455

[a] Molar extinction coefficient at 361 nm for M-9-A and 362 nm for fatty acid probes. The error is the standard deviation for triplicate measurements.

[b] Fluorescent lifetimes in dimyristoyl phosphatidylcholine were for liposomes suspended in H_2O at 20°C. Standard deviation of lifetime measurements was ± 0.7 ns.

[c] Quantum yields relative to quinine sulphate in 0.5 M H_2SO_4 ($Q = 0.546$).

[d] As for c but for probes in egg phosphatidylcholine liposomes suspended in H_2O.

[e] Wavelength of emission maximum.

[f] Liposomes of egg phosphatidylcholine or dimyristoyl phosphatidylcholine suspended in H_2O.

molar volume) reflecting the smaller molar volume and shorter rotational relaxation time of this molecule.

The position of the emission maximum is often used as an indicator of the polarity and structure of the environment surrounding the fluorophore [7]. Table III compares the emission maxima of the probes in water, methanol, hexane and liposomes. The results in water were variable and concentration dependent, and may be affected by micelle formation as indicated by the blue shift relative to methanol [9]. A greater blue shift was observed in hexane. In liposomes (egg phosphatidylcholine or dimyristoyl phosphatidylcholine), a blue shift in the emission maximum was observed as the fluorophore was moved deeper into the hydrophobic interior of the bilayer, the biggest difference occurring between 2-AP and 6-AS. However, M-9-A has an emission maximum red shifted compared to 2-AP despite its location in the centre of the bilayer (see below). In methanol or hexane the emission maximum of all probes is similar and shows no trend.

Quantum yields. Table III shows that the yields in methanol are similar indicating that the intrinsic quantum yield is independent of the position of the fluorophore along the acyl chain. However, in liposomes the quantum yield increases as the fluorophore is moved deeper into the bilayer as would be expected for a polarity gradient from the surface to the centre of the bilayer. Again, M-9-A does not fit this pattern but gives a lower quantum yield than expected for its position at the bilayer centre.

Lifetimes. The response of the emission maximum and quantum yield to a polarity gradient is also seen in the values of the fluorescent lifetimes which increase from 7.7 ns for 2-AP to 10.4 ns for 12-AS (Table III).

Location of the probes in the bilayer

The relative location of the probes in the bilayer was determined by measuring the relative quenching efficiencies of three different quenching agents on each of the five probes bound to dimyristoyl phosphatidylcholine liposomes.

Copper (II). We may expect that the quenching of the probes by a paramagnetic quenching agent (Cu(II) either in the aqueous phase or bound to the membrane surface would reflect the accessability of the fluorophores in the bilayer. The results analysed according to the Stern-Volmer equation are depicted in Fig. 4. We note that these plots are non-linear and we have shown earlier that this behaviour can arise in cases when the concentration of total rather than bound quencher is used on the abscissa axis *. Nevertheless, it is clear that the quenching efficiencies, as reflected by the slope of the line at [Cu(II)] $\rightarrow$ 0, are in the order 2-AP > 6-AS > 9-AS > 12-AS > M-9-A. Values of the biomolecular quenching constants calculated from these initial slopes are listed in Table IV and are indicative of a diffusion-controlled process [22].

The double reciprocal plot of the quenching data is presented in Fig. 5. The plots for 6-, 9- and 12-AS have a common ordinate intercept indicating that the same degree of quenching is achieved at infinite concentration of quencher.

* Non-linear plots of this type also arise in situations where fluorophores are arranged within a macrostructure such that only a certain proportion of them is accessible to the quencher, e.g. tryptophan residues in a protein. The theory for this situation has been described by Lehrer [36].

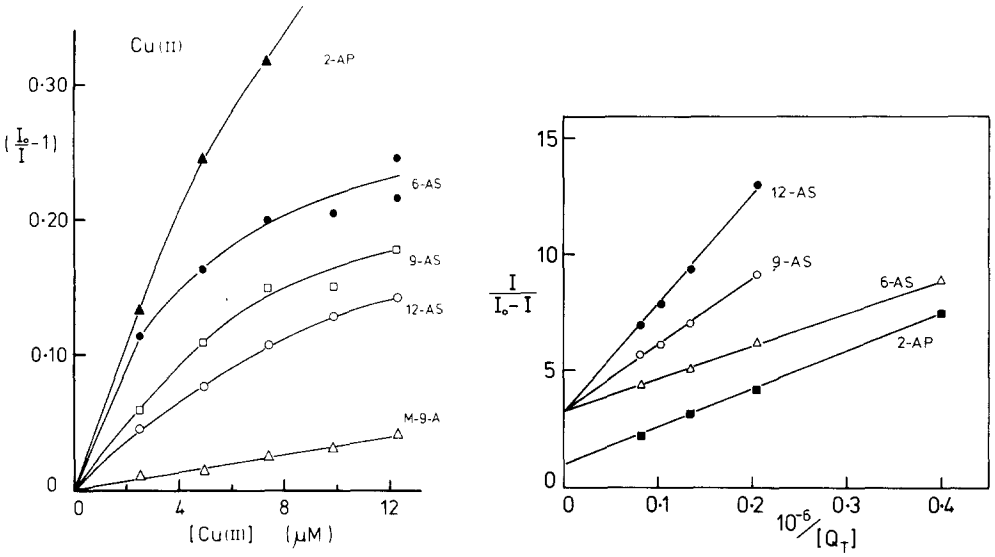

Fig. 4. Stern-Volmer plots for the quenching of fluorescent probes in dimyristoyl phosphatidylcholine liposomes by Cu(II).

Fig. 5. Data in Fig. 4 plotted in double reciprocal form to Eqn. 10.

The plot of 2-AP is distinctly different having a lower ordinate intercept suggesting that a different process is involved in the quenching of this fluorophore. Values of the apparent equilibrium constant for the Cu(II) binding calculated according to Eqn. 10 are presented in Table IV.

N,N-Dimethylaniline. Dimethylaniline is an efficient quencher of anthracene fluorescence [23]. Because of its hydrophobic nature we would expect it to enter the bilayer and locate near the centre of the bilayer. We would therefore expect the relative quenching efficiencies of the five probes to be in the reverse order to that observed for quenching by surface-bound Cu(II). Fig. 6 shows that this indeed is the case except that 2-AP is out of sequence and has a quenching efficiency closer to that for 9-AS.

16-Nitroxide stearic acid. In dimyristoyl phosphatidylcholine liposomes we

TABLE IV

VALUES OF THE APPARENT BIMOLECULAR QUENCHING CONSTANT (k_q) AND THE APPARENT ASSOCIATION CONSTANT (K_A) FOR THE BINDING OF Cu(II) TO DIMYRISTOYL PHOSPHATIDYLCHOLINE LIPOSOMES

The data is derived from Figs. 4 and 5 as outlined in Theory.

Probe	$k_q \times 10^{-9}$ ($M^{-1} \cdot s^{-1}$)	$K_A \times 10^{-6}$ (M^{-1})
2-AP	2.29	0.07
6-AS	1.69	0.23
9-AS	0.83	0.11
12-AS	0.60	0.07
M-9-A	0.12	—

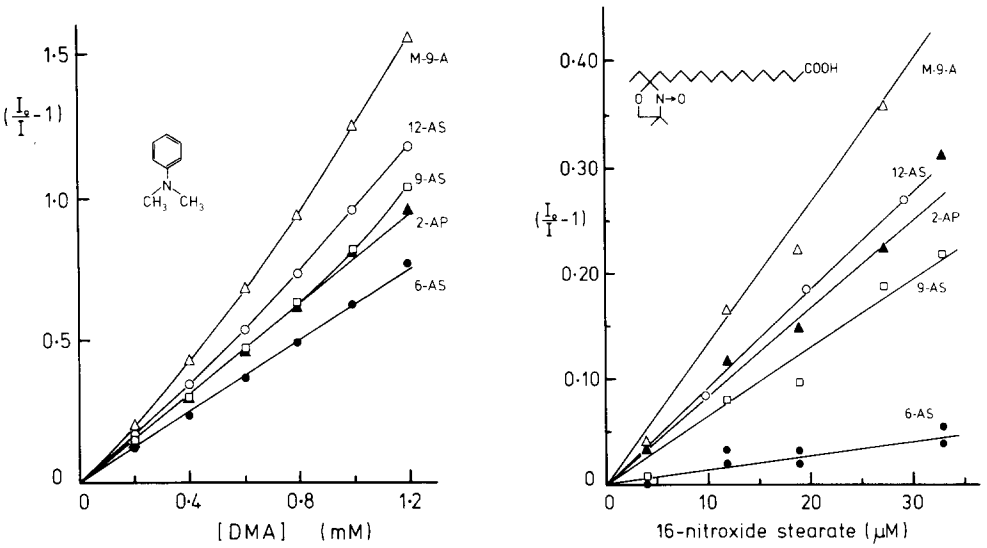

Fig. 6. Stern-Volmer plots for the quenching of fluorescent probes in dimyristoyl phosphatidylcholine liposomes by *N,N*-dimethylaniline.

Fig. 7. Stern-Volmer plots for the quenching of fluorescent probes in dimyristoyl phosphatidylcholine liposomes by 16-nitroxide stearic acid.

would expect the nitroxide ring of this spin-labelled probe to locate near the centre of the bilayer. Quenching of anthracene fluorescence presumably occurs via a paramagnetic mechanism and Fig. 7 shows that the relative quenching efficiencies are in the same order as that observed for quenching by dimethyl-

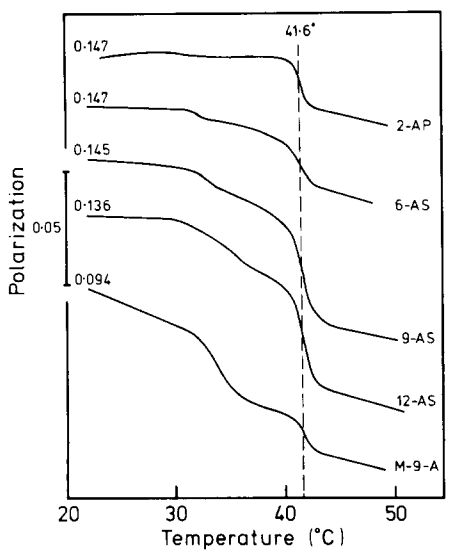

Fig. 8. Continuous recording of polarization versus temperature for the phase transitions of dipalmitoyl phosphatidylcholine. Plots are displaced one beneath the other for ease of presentation. The scale division for polarization is indicated on the ordinate. The figures refer to the relative polarization values at 20°C.

TABLE V

VALUES OF Δp AND $\Delta\rho$ ACROSS THE CRYSTALLINE-LIQUID CRYSTALLINE PHASE TRANSITION OF DIPALMITOYL PHOSPHATIDYLCHOLINE

Values of $\Delta\rho$ for M-9-A are not presented due to uncertainty in the temperature dependence of τ for this probe.

Probe	$L_{\beta'} \rightarrow P_{\beta'}$ (30—38°C)		$L_{\beta'} \rightarrow L_{\alpha}$ (30—44°C)	
	Δp	$\Delta\rho$ (ns)	Δp	$\Delta\rho$ (ns)
2-AP	0.004	2.0	0.026	10.7
6-AS	0.012	3.0	0.056	13.2
9-AS	0.019	5.5	0.071	16.2
12-AS	0.025	7.6	0.077	17.4
M-9-A	0.042	—	0.064	—

aniline. Again 2-AP is out of sequence having a quenching efficiency closer to that for 12-AS.

The dipalmitoyl phosphatidylcholine phase transition

To demonstrate the application of the fluorescent probes we have examined the crystalline-liquid crystalline phase transition of dipalmitoyl phosphatidylcholine. Plots of polarization versus temperature are presented in Fig. 8. All probes sense the main transition at 41.6°C. The sensitivity of the fluorophore to the pretransition appears to increase as the probe is placed deeper into the bilayer. A similar set of curves is found when the rotational relaxation time is plotted against temperature. We have used the change in p and ρ between 30 and 38°C ($\Delta p_{30-38°C}$ and $\Delta\rho_{30-38°C}$) as indicative of the magnitude of the changes occurring during the pretransition ($L_{\beta'} \rightarrow P_{\beta'}$) *. These values are presented in Table V and show that the pretransition involves a greater change in microviscosity at the centre of the bilayer than at the surface. Table V also present values of Δp and $\Delta\rho$ across the whole transition ($L_{\beta'} \rightarrow L_{\alpha}$, $\Delta p_{30-44°C}$ and $\Delta\rho_{30-44°C}$). These results also show that from the gel to the fluid state ($L_{\beta'} \rightarrow L_{\alpha}$) the greatest changes in microviscosity occur towards the centre of the bilayer.

Discussion

The presence of impurities in the probe preparations can be adequetely detected by measuring spectral characteristics (infrared and ultraviolet absorption, fluorescence emission) and by thin-layer chromatographic analysis. In solvents such as methanol or hexane the fluorescent characteristics (quantum yield, lifetime, p_0) of the fatty acid probes are similar (Table III) indicating that the position of the anthracene ring on the acyl chain does not cause intrinsic differences in these parameters. However, when the probes are placed in an anisotropic environment, namely a phospholipid bilayer, significant differences

* The nomenclature adopted is that of Luzzati [37].

are found in the lifetime, quantum yield and in the position of the emission maximum. In each case, the data indicate that the fluorophore enters a less polar enviroment the deeper it is buried into the bilayer. We believe that the most accurate measure of this trend is the position of the emission maximum and we note that the largest blue shift in λ_{max} occurs between 2-AP and 6-AS suggesting that little water penetrates past the 6-AS position. This observation is in agreement with the results of Griffith et al. [24] for spin-labelled fatty acids. We note that the trends discussed above may be less pronounced than expected since the decreased restraint on solvent rearrangement toward the bilayer centre (i.e. decreased viscosity) can lead to decreased quantum yields and often to shorter excited state lifetimes [6]. The spectral properties reported in Table III for 2-AP and 12-AS are in general agreement with published data [9,10].

The use of quenching reagents which locate at the surface or the centre of the bilayer have proved useful to establish the relative position of the fluorophores. The use of Cu(II) results in non-linear Stern-Volmer plots (Fig. 4) and we have shown that such plots are to be expected when a quencher binds to the bilayer surface. The relative quenching efficiencies are best indicated by the values of the apparent bimolecular quenching constants listed in Table IV. The simplest explanation of these results is that the deeper fluorophores are less acesssible to quencher. This implies that the bilayer is to some extent permeable to Cu(II) (perhaps in the form of $CuSO_4$) since paramagnetic quenching is believed to require close contact between fluorophore and quencher (4—6Å [25,26]). It is possible therefore that a gradient of Cu(II) exists from the surface to the centre of the bilayer. This interpretation is supported by the following considerations.

The double reciprocal plot of the Cu(II) quenching data (Fig. 5) suggests that the mechanism of quenching differs from 2-AP on one hand and for 6-, 9- and 12-AS on the other. In the former case, Cu(II) bound at the bilayer surface could be sufficiently close to the anthracene ring to cause significant paramagnetic quenching. The binding of divalent cations to phosphatidylcholine is very weak [27,28] and is insufficient to explain the efficient quenching observed. On the other hand, Cu(II) could bind to the carboxyl group of the probe itself so bringing it into close contact with the fluorophore. Indeed, increased quenching of all probes was found for liposomes containing 2 mol% palmitic acid. The deeper probes could be quenched by a gradient of Cu(II) in the bilayer determined by high local concentrations of Cu(II) near the carboxyl group at the bilayer surface. At high concentrations of quencher this gradient would be such that all probes were quenched with equal efficiency as indicated by the common ordinate intercept in Fig. 5. If the quenching had reflected the binding process for the 6-, 9- and 12-AS probes we would have expected the apparent binding constant to be similar in each case and the ordinate intercepts would have differed due to different values of K_A and τ (Eqn. 10). Such is not the case (Fig. 5, Table IV). An explanation based on the influence of microviscosity on the rate of a diffusion-controlled process is unacceptable since it predicts that quenching would be more efficient towards the centre of the bilayer where the microviscosity is lower.

The relative positions of the fluorophores are also confirmed by the quench-

ing data obtained for *N,N*-dimethylaniline and 16-nitroxide stearic acid. In these cases the theory is more complicated since both partition and binding processes may be involved in the uptake of these molecules into the bilayer. We believe that the misplacement of 2-AP in the series for both these quenchers (Figs. 6 and 7) arises because a certain proportion of material may reside in the aqueous phase depending on the partition coefficient and/or binding constants involved. For example, ESR experiments have shown that 16-doxylstearate has appreciable water solubility [29]. Thus the surface probe (2-AP) is quenched by molecules in both lipid and aqueous phases.

While these quenching experiments indicate the relative position of the probes in the bilayer, some indication of the absolute positions of the fluorophores comes from the recent work of Podo and Blasie [30] who examined the PMR spectra of dipalmitoyl phosphatidylcholine vesicles containing 2-AP and 12-AS. Chemical shifts were seen in the region of the terminal methylene protons for 12-AS, whereas 2-AP affected shifts near the first and second methylene groups of the acyl chains indicating that its fluorophore was located level with the carbonyl group of the ester linkage. Our data confirms the location of 6-AS and 9-AS between these positions.

Continuous recording of polarization and intensity during the dipalmitoyl phosphatidylcholine phase transition improves the accuracy of this measurement [9]. All probes register the pretransition and the main transition. The results indicate that the pretransition involves a greater change in microviscosity at the centre of the bilayer than at the surface (Fig. 8, Table V). The pretransition represents a greater proportion of the total change in microviscosity from gel to fluid state as the fluorophore is placed deeper in the bilayer. This information may be added to that obtained from recent X-ray diffraction experiments which indicates that the pretransition is associated with a structural transformation from a "one-dimensional lamellar to a two-dimensional monoclinic lattice consisting of lipid lamellae distorted by a periodic ripple" [31]. It is also true that over the complete crystalline-liquid crystalline transition the changes are greater at the bilayer centre that at the surface (Table V). In this connnection, the ESR data of Marsh [32] is of interest since it shows that there is a greater change in the ESR order parameter for spin-labelled fatty acids as the nitroxyl group is moved along the acyl chain and therefore deeper in the bilayer. However, it would appear that sonicated dispersions which do not show a pretransition were used in these experiments.

During these measurements of the phase transition it became clear that the behaviour of M-9-A differed markedly from that of the fluorescent fatty acid probes. In particular, large increases in fluorescence intensity were observed during both the pretransition and the main transition of dipalmitoyl phosphatidylcholine and it was evident that the intensity could not be used to monitor changes in fluorescence lifetime. Hence values of ρ for this probe have been omitted from Table V. The results suggested that there was a significant increase in the binding and/or partition of M-9-A into the membrane as the bilayer became more fluid. Similar behaviour has been observed for *N*-phenylnaphthylamine [33] and for the spin label TEMPO [34]. On the other hand binding experiments have indicated that the fluorescent fatty acids are completely bound to the membrane under the conditions used in the transition experiments described.

Recently, Cadenhead et al. [35] have studied the perturbation of bilayer structure by 2-AP, 12-AS and 16-AS using surface balance, differential scanning calorimetry and fluorescence polarization techniques. While agreeing with the main features of their fluorescence results we have not been able to show any differences in the temperature of the main transition between the four fatty acid probes. Indeed, the transition temperature was independent of probe concentration within the concentration range commonly employed (probe to lipid ratios 1 : 150—1 : 500). In addition, the fluidity gradient as determined by the fluorescent fatty acids agrees well with that determined by a non-perturbing technique [11]. Perturbation of bilayer structure in terms of changes in fluorescent parameters at low probe concentration therefore appears to be minimal. On the other hand perturbation may be detected by more sensitive techniques such as the measurement of membrane conductance (Thulborn et al., manuscript in preparation).

In this paper we have reported the properties of a set of fluorescent probes sensitive to the fluidity gradient of the lipid bilayer. Their relative positions in the bilayer have been established and we have demonstrated their use by examining the structural changes which occur during the phase transition of a pure phosphatidylcholine. More recently we have found that these probes indicate that a microviscosity barrier exists in bilayers of unsaturated phosphatidylcholines such that above and below the region of the double bonds there is a significant decrease in microviscosity [11]. The probes described offer a relative simple method for monitoring bilayer structure and the penetration of various membrane components.

Acknowledgements

We thank Jim Potter and Robert Goullet for assistance with the construction of the fluorescence polarization instrument, Ray Robbins for supplying the deconvolution program and John Raison for the sample of the nitroxide stearic acid. We are grateful to Edward Treloar for assistance with the measurements of fluorescence lifetime. K.R.T. is the recipient of a Commonwealth Postgraduate Research Award. The work was supported by the Australian Research Grant Commision.

References

1 Lee, A.G. (1975) Prog. Biophsy. Mol. Biol. 29, 3—56
2 Seelig, A. and Seelig, J. (1974) Biochemistry 13, 4839—4845
3 Lee, A.G., Birdsall, N.J.M., Metcalfe, J.C., Warren, G.B. and Roberts, G.C.K. (1976) Proc. R. Soc. Lond. Ser. B. 193, 253—274
4 Hubbell, W.L. and McConnell, H.M. (1971) J. Am. Chem. Soc. 93, 314—326
5 Kaplan, J., Canonico, P.G. and Caspary, W.J. (1973) Proc. Natl. Acad. Sci. U.S. 70, 66—70
6 Radda, G.K. (1975) in Methods in Membrane Biology (Korn, E.D., ed.), Vol. 4, pp. 97—188, Plenum Press, New York
7 Azzi, A. (1975) Q. Rev. Biophys. 8, 237—316
8 Lentz, B.R., Barenholz, Y. and Thompson, T.E. (1976) Biochemistry 15, 4521—4528
9 Bashford, C.L., Morgan, C.G. and Radda, G.K. (1976) Biochim. Biophys. Acta 426, 157—172
10 Waggoner, A.S. and Stryer, L. (1970) Proc. Natl. Acad. Sci. U.S. 67, 579—589
11 Thulborn, K.R. Sawyer, W.H. and Treloar, F.E. (1978) Biochem. Biophys. Res. Commun., in the press
12 Robles, E.C. and Van den Berg, D. (1969) Biochim. Biophys. Acta 187, 520—526

13 Lawaczek, R., Kainosho, M. and Chan, S.I. (1976) Biochim. Biophys. Acta 443, 313–330
14 Perrin, F. (1926) J. Phys. Radium. 7, 390–401
15 Weber, G. and Daniel, E. (1966) Biochemistry 5, 1900–1907
16 Hare, F. and Lussan, C. (1977) Biochim. Biophys. Acta 467, 262–272
17 Parker, C.A. and Rees, W.T. (1960) Analyst 85, 587–600
18 Lenard, J., Wong, C. and Compans, R.W. (1974) Biochim. Biophys. Acta 332, 341–349
19 Parish, R.C. and Stock, L.M. (1965) J. Org. Chem. 30, 927–929
20 Stern, O. and Volmer, M. (1919) Phys. Z. 20, 183–190
21 Klotz, I.M. (1946) Arch. Biochem. 9, 109–117
22 Parker, C.A. (1968) Photoluminescence of Solutions, p. 74, Elsevier
23 Saltiel, J., Townsend, D.E., Watson, B.D., Shannon, P. and Finson, S.L. (1977) J. Am. Chem. Soc. 99, 884–896
24 Griffith, O.H., Dehlinger, P.J. and Van, S.P. (1974) J. Membrane Biol. 15, 159–192
25 Green, J.A., Singer, L.A. and Parks, F.H. (1973) J. Chem. Phys. 58, 2690–2695
26 Bieri, V.G. and Wallach, D.F.H. (1975) Biochim. Biophys. Acta 389, 413–427
27 Misiorowski, R.L. and Wells, M.A. (1973) Biochemistry 12, 967–975
28 Puskin, J.S. (1977) J. Membrane Biol. 35, 39–55
29 Wallach, D.F.H., Verma, S.P., Weidekamm, E. and Bieri, V. (1974) Biochim. Biophys. Acta 356, 68–81
30 Podo, F. and Blasie, J.K. (1977) Proc. Natl. Acad. Sci. U.S. 74, 1032–1036
31 Janiak, M.J., Small, D.M. and Shipley, G.G. (1976) Biochemistry 15, 4575–4580
32 Marsh, D. (1975) Essays Biochem. 11, 139–180
33 Trauble, H. and Overath, P. (1973) Biochim. Biophys. Acta 307, 491–512
34 Hubbell, W.L. and McConnell, H.M. (1968) Proc. Natl. Acad. Sci. U.S. 61, 12–16
35 Cadenhead, D.A., Kellner, B.M.J., Jacobson, K., and Papahadjopoulos, D. (1977) Biochemistry 16, 5386–5392
36 Lehrer, S.S. (1971) Biochemistry 10, 3255–3263
37 Luzzati, V. (1968) Biol. Membranes 1, 71–123, Academic Press, New York